Available online at www.sciencedirect.com
ScienceDirect
Journal of Power Sources 174 (2007) 1241–1250
JOURNAL OF POWER SOURCES
www.elsevier.com/locate/jpowsour

More on the performance of $LiFePO_4$ electrodes—The effect of synthesis route, solution composition, aging, and temperature

M. Koltypin [a], D. Aurbach [a,*], L. Nazar [b], B. Ellis [b]

[a] *Department of Chemistry, Bar-Ilan University, Ramat-Gan 52900, Israel*
[b] *Department of Chemistry, University of Waterloo, Waterloo, Canada*

Available online 23 June 2007

Abstract

Three types of olivine compounds were prepared by three different routes: sol–gel, solid-state, and hydrothermal syntheses, showing the expected structure and containing a small amount of carbon and iron phosphide for maintaining sufficient intrinsic electrical conductivity. These materials were tested in $LiClO_4$, and in dry and wet $LiPF_6$ solutions in mixtures of ethylene and dimethyl carbonate (EC–DMC, 1:1) at 30 and 60 °C. Iron dissolution from these materials, upon storage in the three solutions at these two temperatures, was measured by ICP. Aged electrodes were measured by XRD and SEM: the electrochemical performance of the three types of olivine compounds in the three solutions and at the two temperatures was measured by voltammetry and impedance spectroscopy. The behavior of pristine and aged electrodes was systematically compared. It was found that there is a strong correlation between the rate of iron dissolution and the performance of these systems in terms of high capacity, low capacity fading, and low and stable impedance upon aging. The material prepared by sol–gel synthesis demonstrated a low iron dissolution rate, even in a corrosive solution such as wet $LiPF_6$ solutions, and high performance, even in these solutions. When the solutions contain no acidic contaminants, all the compounds demonstrated negligible iron dissolution rates, even at 60 °C, and a good electrochemical performance. The electrochemical comparison described herein shows a pronounced impact of the solution composition on the electrodes' impedance, due to the unique surface chemistry developed in each solution.

Keywords: $LiFePO_4$; $LiPF_6$ solutions; EIS; Voltammetry; Aging

1. Introduction

In the search for new positive electrode materials for lithium-ion batteries, research has concentrated on developing inexpensive, environmentally benign and safe materials that can also meet the demands of high-rate devices. With respect to the first two criteria, layered lithium metal oxides such as $LiMnO_2$ and $LiFeO_2$ have been intensively investigated. However, $LiMnO_2$ is difficult to prepare in its layered form and converts to the spinel upon cycling [1]. $LiFeO_2$ shows little ability for lithium extraction due to the difficulty in accessing the Fe^{4+}/Fe^{3+} couple [2]. Hence, several compounds have been explored as possible alternatives, especially those obtained by introducing large polyanions of the form $(XO_4)^{y-}$ (X = S, P, As, Mo, W; $y = 2$ or 3) into the lattice. This approach came to prominence in 1997, radically changing the focus of the lithium battery community, when Goodenough's group determined that $(PO_4)^{3-}$ and $(SO_4)^{2-}$ polyanions stabilize the structure and raise redox energies, compared to those in oxides [3]. In the case of iron, the phosphate and sulfate compounds display potentials in the range of 2.8–3.6 V *versus* Li/Li^+. The presence of the polyanion $(XO_4)^{y-}$ with strong X–O covalent bonds stabilizes the metal (M) antibonding state, which is accomplished through an M–O–X inductive effect that has now been thoroughly studied for many transition metal phosphates. Currently, lithium transition metal phosphates such as $LiFePO_4$ [4], $LiMnPO_4$ [5], $Li_3V_2(PO_4)_3$ [6], and $LiVPO_4F$ [7] have all been recognized as exciting positive electrodes for these systems because of their energy storage capacity combined with electrochemical and thermal stability. Among these, the olivine $LiFePO_4$ has exhibited the most promising properties (and is also found in nature as the mineral triphylite). It is made from amply-available elements, thus reducing the potential cost of production of this compound, which has a theoretical capacity of 170 mAh g^{-1}.

This very well studied structure adopts an orthorhombic lattice with the space group P_{nma} (#62) and reported lattice

* Corresponding author.
E-mail address: aurbach@mail.biu.ac.il (D. Aurbach).

0378-7753/$ – see front matter © 2007 Elsevier B.V. All rights reserved.
doi:10.1016/j.jpowsour.2007.06.045

parameters of typically $a = 10.333$ Å, $b = 6.004$ Å, and $c = 4.692$ Å. Each unit cell accommodates four $LiFePO_4$ formula units. There are two unique octahedral sites in the olivine structure: the M1 site (occupied by the lower valent cation) and the M2 site, occupied by the higher valent cation. Structural calculations have shown that for olivines consisting of two metals of different valences (Li^+ and Fe^{2+} in $LiFePO_4$, for example), there is no mixing of the constituents of these octahedral sites [8]. The synthesis of $LiFePO_4$ at low temperature has, however, been reported to lead to some disorder, leading to poor electrochemical performance [9]. The M1 sites form linear chains of edge-sharing octahedra along the direction of the *b*-axis, while the M2 sites form staggered chains of corner-shared octahedra, also in the direction of the *b*-axis. These chains are bridged by edge- and corner-shared phosphate tetrahedra, creating a stable three-dimensional structure.

The electronically insulating effect of the phosphate groups on which the inductive effect relies results in the isolation of the redox centers within the lattice, and increases the band gap *vis-à-vis* the oxide to values that are in the range of 3.7 eV in $LiFePO_4$, based on both calculations and experiments [10]. Electron transport in this very poor semiconductor ($\sigma \sim 10^{-9}$ S cm^{-1}) is dependent upon the small polaron hopping of Fe^{3+} holes within the lattice. Recent calculations predict an activation energy of 0.185 eV for a "free polaron" carrier in the absence of ionic interactions [11]. The consequence of electronic transport limitation has led to significant efforts to overcome it, including methods to coat the phosphate particles with carbon [12], to embed them in a carbon matrix [13] and lay down metal particles to form a composite [14].

Since such surface structures can only partially solve the transport problem, a key issue in these materials is to disentangle the factors governing ion and electron transport within the lattice. For example, calculations of "free" ion transport suggest that the ion mobility along the M1 chain direction is high (10^{-8} cm^2 s^{-1} [15], similar to that calculated and determined for $LiCoO_2$ [16]), but the material does not exhibit the properties of a fast ion conductor [9]. Important to this is the creation of solid solutions over a wide lithium concentration range to facilitate coupled ion and electron transport. In the $LiMPO_4$ family of materials, the extraction of lithium forms a two-phase $LiMPO_4/MPO_4$ mixture that is, in part, driven by the volume change between the structures. The solubility of the two phases at room temperature is not accurately known. Some reports suggest a pure two-phase coexistence with no mutual solubility [17], whereas others give evidence for very narrow single-phase regimes, $Li_\alpha FePO_4$ and $Li_{1-\beta}FePO_4$ [18,19]. Very recently, neutron diffraction data have been reported, which claim a somewhat wider region of solid solution at room temperature, with α and $1 - \beta$ of 0.05 and 0.89, respectively [20]. Naturally, in the absence of any solid solution domains, lithium-ion extraction, and Li^+-ion transport within the pure parent members are difficult to explain. Nonetheless, the very limited solubility is probably responsible for the electrochemical limitations of the material owing to the low intrinsic ionic and electronic conductivity, and hence, the low mobility of the phase boundary. However, it was recently demonstrated that a transition to a Li_xFePO_4 solid solution (SS) phase occurs at about or above 485 K, where lithium occupation is random within the lattice [21]. The onset temperature of electron delocalization is also correlated to the state of lithium disorder, suggesting that the two transport mechanisms are coupled [22]. Thus, the transport is limited not by carrier alone, but by their concerted mobility through the lattice.

The limited phase solubility, and coupled ion/electron transport, makes the electrochemical response fascinating to study by transients. However, because the transition between $LiFePO_4$ and $FePO_4$ is essentially a first-order phase transition, standard electrochemical tools may not be applicable to a wide potential range. In particular, although a strong correlation between structure and rates has been established, what has not yet been explored, relates to behavior at high temperature.

In this work, we examined the effect of the synthetic route, solution composition, temperature, and aging, on the performance of $LiFePO_4$ electrodes. Olivine compounds were prepared by sol–gel, solid-state, and hydrothermal synthetic routes. $LiClO_4$ solutions were chosen as electrolyte systems containing no acidic species. Dry and wet $LiPF_6$ solutions were tested as standard and pronouncedly contaminated solutions, containing acidic species (HF). Electrodes were measured soon after contact with the electrolyte solutions (pristine), and after aging during 2–3 weeks at 30 and 60 °C. ICP, XRD, and SEM were applied in conjunction with standard electrochemical techniques.

2. Experimental

The $LiFePO_4$ materials used in this work were prepared by three different routes:

1. Sol–gel synthesis: $LiFePO_4$ was prepared by a sol–gel method using Li_3PO_4, phosphoric acid ($0.85H_3PO_4 \cdot 0.15H_2O$) and ferric citrate *n*-hydrate ($FeC_6H_8O_7 \cdot nH_2O$) as starting materials. Lithium phosphate (0.03 M) and phosphoric acid (0.06 M) were dissolved in 200 ml of water. Ferric citrate *n*-hydrate (0.09 M) was dissolved in 500 ml of boiling water, and the two solutions were combined and concentrated on a hot plate until a wet gel with high viscosity was formed. The wet gel was placed in an oven and heated at 140 °C for 12 h. The dried gel was ground before firing at a heating rate of 10 °C min^{-1} under Ar up to 600 °C, held for 24 h, and the samples were then air quenched to obtain crystallized $LiFePO_4$. The final product contains 5% carbon and 4% iron phosphide. Carbon content was determined by chemical analysis, and the iron phosphide contribution was estimated by Mossbauer analysis [23].
2. Solid-state synthesis: The reaction mixture comprised $FeC_2O_4 \cdot 2H_2O$, $NH_4H_2PO_4$, and $0.5Li_2CO_3$ that were combined in stoichiometric molar amounts. The reaction mixture was ball milled in silicon nitride media for 2 h, then fired at 600 °C under nitrogen, followed by heating at 700 °C under 7% H_2/N_2 during 30 min. The final product contains 1% carbon and 2% Fe_2P.
3. Hydrothermal synthesis: The reagents H_3PO_4, $(NH_4)_2Fe(SO_4) \cdot 6H_2O$, $3LiOH \cdot H_2O$, and ascorbic acid were placed

in an 45 ml Parr autoclave, and the container was filled to 67% with distilled water. The autoclave was heated to 190 °C for 5 h, and then cooled. The product was isolated by filtration, and fired at 600 °C for 6 h under Ar. The final product contains 1.8% carbon. None of the pristine powders contained any Fe^{3+} compound. The only contamination in the as synthesized materials includes carbon and/or iron phosphide, as specified above.

The composite electrodes contained $LiFePO_4$ as the active mass (≈80% by weight), carbon black, an additional conductive additive, and a polyvinylidene difluoride (PVdF) binder (≈10% each by weight) on Al foil current collectors. For the spectroscopic measurements, we used electrodes comprising aluminum foil in which $LiFePO_4$ particles were embedded by pressure. $LiFePO_4$ powder was pressed onto the foil by a hydraulic press. The exact load of the active mass per cm^2 could be easily measured by weight. Two- and three-electrode coin-type cells were prepared under highly pure Ar atmosphere in VAC Inc. glove boxes, using standard 2032 cells from NRC Inc. (Canada), in which metallic lithium foils were used as counter and reference electrodes. Their preparation is described elsewhere [24].

The electrolyte solutions included 1 M $LiClO_4$ and 1 M $LiPF_6$ in EC–DMC 1:1 mixtures, Li battery grade, from Merck Inc. and Tomiyama Inc., and could be used as received. We also used $LiPF_6$ solutions that were deliberately contaminated by 100 ppm of water. Storage and electrochemical measurements were carried out at 30 and 60 °C using the appropriate thermostats.

The techniques and instrumentation included elemental analysis by inductively coupled plasma (ICP), by an Ultima 2, Jobin-Yvon-Horiba spectrometer; a FTIR spectrometer from Nicolet Inc. (Magna 860), placed in an H_2O- and CO_2-free atmosphere in a glove box, in reflectance mode; an HAxis XPS system from Kratos; a SEM (JSM-840) from Jeol Inc.; a D8 Advance X-ray diffractometer from Bruker and standard electrochemical techniques (voltammetry and EIS) using a Solartron Inc. multichannel system, model 1470A; and a frequency response analyzer (FRA), model 1255, from the same company. For iron dissolution tests, 50–100 mg of the olivine compound was stored in closed vials containing 1 ml of an electrolyte solution under Ar atmosphere. The solution was removed after a period of storage at 30 or at 60 °C and was analyzed by ICP for the presence of iron. Electrodes comprising $LiFePO_4$ powder on Al foil were treated electrochemically in coin-type cells. The electrodes (containing no additives) were removed from the electrolyte solution, washed several times with highly pure THF, and were transferred under a pure Ar atmosphere to the FTIR or the XPS spectrophotometers. The FTIR measurements were carried out in reflectance mode using a grazing angle attachment (FT80) from Spectratech Inc. The electrodes were sufficiently reflective to provide a valuable spectral response. A nickel mirror was used for the reference spectra. Samples of XPS were transferred from the glove box (highly pure At atmosphere) to the high vacuum system of the spectrometer, using a home made transfer system that contains a magnetic manipulator and a gate valve. (The samples cannot be exposed to atmospheric gases, except for the impurities in the glove box atmosphere that are at the ppm level.)

3. Results and discussion

The scope of studies described herein includes a matrix of three types of $LiFePO_4$ olivine compounds synthesized by three different methods: sol–gel, solid-state, and hydrothermal syntheses (see Section 2), three electrolyte solutions based on EC–DMC (1:1) mixtures that differ from each other by the amount of acidic/protic contaminants, by the choice of salt and the level of water contamination, and two temperatures, 30 and 60 °C. The $LiClO_4$ solutions used herein can be considered as uncontaminated solutions (H_2O contamination below 10 ppm), since $LiClO_4$ can be purified very easily by heating it in vacuum. This salt does not bring with it any acidic contaminations to the solution. In contrast, $LiPF_6$ solutions always contain traces of HF (can reach several hundreds of ppm [25]). $LiPF_6$ decomposes to LiF and PF_5 at elevated temperatures [26]. The latter reacts readily with any protic moiety to form HF (e.g., $PF_6 + H_2O \rightleftharpoons 2HF + POF_3$). We used herein two types of 1 M $LiPF_6$ solutions, a regular standard one (the same that is currently used in Li-ion batteries), and a solution contaminated by 100 ppm of water. Both solutions should be considered as 'corrosive' for lithiated transition metal oxides (i.e., transition metal ions from the oxide are dissolved in the solutions, followed by possible surface and/or bulk changes in the active mass), as was clearly demonstrated [27]. Samples of $LiFePO_4$ synthesized by the three different methods were stored in $LiClO_4$, $LiPF_6$, and $LiPF_6$/100 ppm H_2O solutions at 30 and 60 °C. The iron dissolution from these samples upon storage was measured by ICP analysis to the solutions. Note that in these experiments about 100 mg of sample was stored in 1 ml of solution. This means that there is a very high ratio between the solution and the sample masses, which may be orders of magnitude higher than those in practical batteries, but ensure a clear distinction between the effect of the sample type, solution, and temperature on the rate of iron dissolution.

Table 1
Percent of iron dissolution from $LiFePO_4$ powders after 20 days of storage in the three solutions indicated, at 30 and 60 °C

Synthesis	$LiClO_4$ 1 M EC/DMC		$LiPF_6$ 1 M EC/DMC		$LiPF_6$ 1 M EC/DMC + 100 ppm H_2O	
	30 °C	60 °C	30 °C	60 °C	30 °C	60 °C
Sol–gel synthesis	0.2	0.7	1.6	2.7	3.3	5.3
Solid-state synthesis	0.5	1.4	2.2	1.8	4.5	42.4
Hydrothermal synthesis	0.4	0.6	1.5	37.6	5.3	65.9

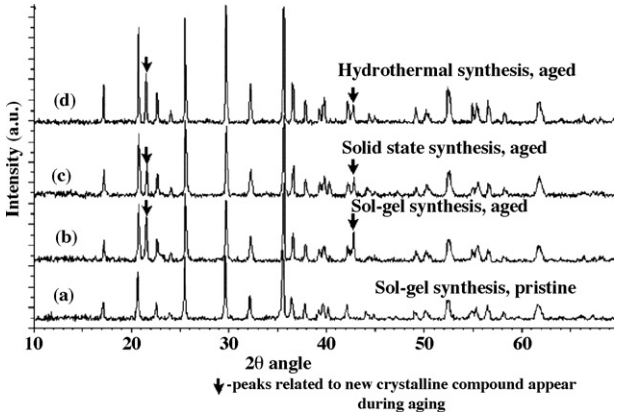

Fig. 1. XRD patters of $LiFePO_4$ powders. (a) Pristine material prepared by a sol–gel synthesis. (b and c) Powders measured after aging during 2 weeks in 1 M $LiPF_6$ EC–DMC (1:1) solutions. The synthetic route is indicated near each pattern, and the arrows mark new pronounced peaks that appear after storage. The XRD patters of all the pristine materials are very similar to pattern (a).

Table 1 shows the percentage of iron dissolution after 20 days of the samples' storage in solutions, as a function of the type of sample (i.e., its synthesis method), solution and temperature. The data in this table reflect the clear effect of the type of sample, solution and temperature on Fe dissolution from these compounds. For all the samples, Fe dissolution was negligible in $LiClO_4$ solutions, even at elevated temperatures. Significant Fe dissolution was always observed in the water-contaminated $LiPF_6$ solutions, and was the highest at 60 °C. The dissolution rates of iron in the $LiPF_6$ solutions usually had intermediate values between those of $LiClO_4$ and the water-contaminated solutions. The $LiFePO_4$ produced by sol–gel synthesis seems to be the most stable among the three types of samples examined herein. Samples after storage were examined by several methods, including XRD, SEM, and surface sensitive techniques. Typical results of the surface analysis of $LiFePO_4$ powder after storage in $LiPF_6$ solutions were demonstrated in a parallel publication [28] and some conclusions drawn from these studies will be mentioned later.

Fig. 1 compares XRD patterns of $LiFePO_4$ samples synthesized by the three different methods after aging at 60 °C in $LiPF_6$ solutions with a sample of pristine material, as indicated. The four XRD patterns presented in Fig. 1 are very similar to each other and reflect the typical and well-known structure of $LiFePO_4$ olivine. However, all the patterns of the aged samples show two new reflections at $2\theta = 22°$ and 43° (indicated by arrows in Fig. 1). So far, we have been unable to identify the origin of these new peaks.

As can be seen in Table 1, aging $LiFePO_4$ prepared by hydrothermal synthesis in $LiPF_6$ solutions (dry) at 60 °C can lead to pronounced iron dissolution, which should be accompanied by parallel pronounced changes in the bulk of the material although these are not evident by XRD. Hence, iron dissolution from $LiFePO_4$ may form mostly amorphous phases under these conditions. For instance, one of the possibilities is the dissolution of Fe^{2+} by exchange with H^+, which forms a LiH_2PO_4 phase. Reaction between HF and $LiFePO_4$ can also form H_3PO_4 that may dissolve in the organic solvents.

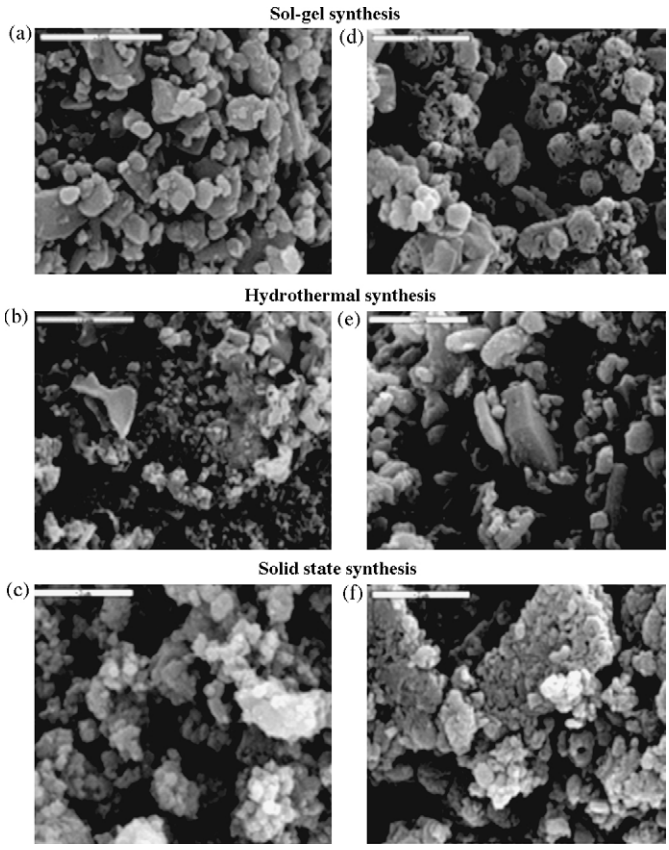

Fig. 2. SEM micrographs of powders prepared by sol–gel (a and d), hydrothermal (b and e) and solid-state (c and f) syntheses, as indicated. The pictures (d–f) relate to powders aged during 2 weeks in dry 1 M $LiPF_6$ solutions. Pictures (a–c) belong to the pristine powders. A scale appears in each picture, corresponding to 2 μm.

Fig. 2 compares SEM micrographs of pristine $LiFePO_4$ powders (synthesized by the three methods) with those of the same powders after aging in $LiPF_6$ solutions at 60 °C. The SEM micrographs of the pristine powder reflect their morphological differences, as expected for materials synthesized from different precursors in different routes. These studies also show some morphological differences between pristine and aged samples. It seems that aging leads to the roughening of the particles' facets. (This is very clear in the comparison between the SEM micrographs of pristine and aged powders prepared by sol–gel and hydrothermal syntheses.) Hence, these morphological studies correlate with iron dissolution from these materials upon aging in $LiPF_6$ solutions at elevated temperatures.

Studies of powders aged in $LiPF_6$ solutions at 60 °C by XPS and FTIR (some data are presented in a parallel publication [28]) showed clearly that surface films are formed on $LiFePO_4$ powders in EC–DMC/$LiPF_6$ solutions at 60 °C, which comprise LiF (obvious detection by XPS, F 1s spectra, a pronounced peak at 685 eV), and organic compounds with carbonyl groups (obvious detection by both XPS and FTIR). To date we have not been able to achieve an exact identification of these organic species. However, they may be alkyl carbonate species formed by nucleophilic attacks on the electrophilic solvent molecules by the negatively charged oxygen at the active mass surface. A similar formation

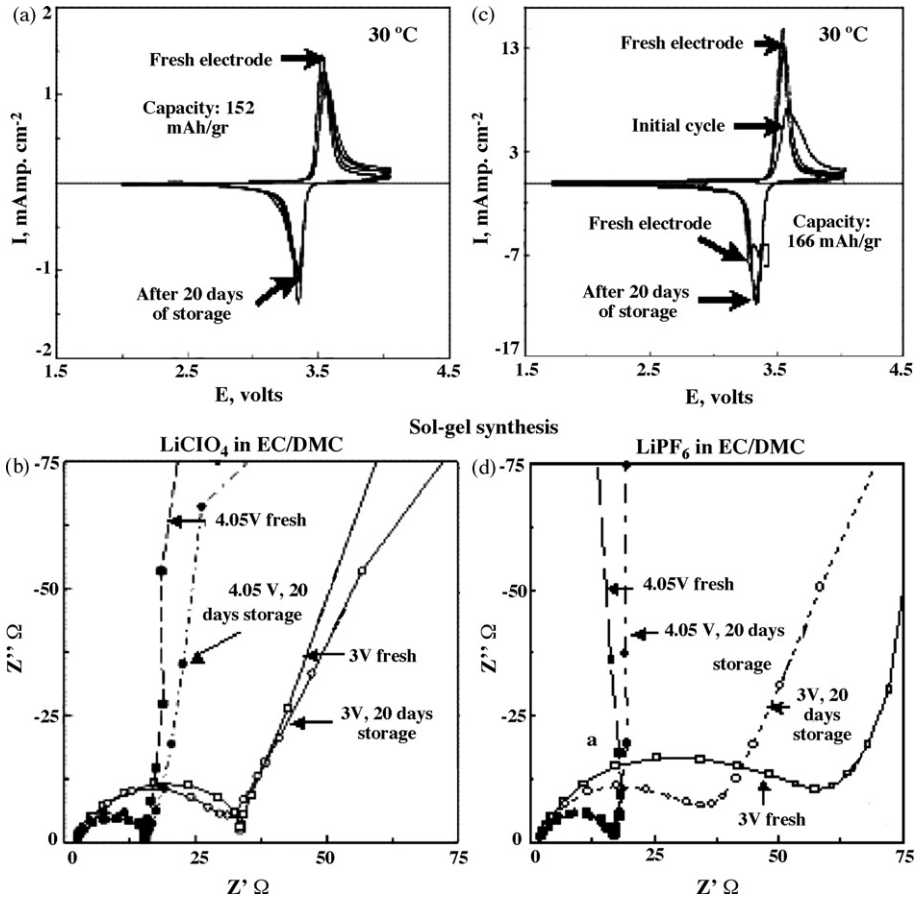

Fig. 3. Electrochemical data related to electrodes comprising $LiFePO_4$ prepared by sol–gel synthesis, measured at 30 °C. (a) Comparison of CVs measured in 1 M $LiClO_4$ solutions from pristine and aged (20 days) electrodes, capacity and scan rate indicated. (b) Impedance spectra measured at 3 and 4.05 V (Li/Li^+) from pristine and aged (20 days) electrodes in $LiClO_4$ solutions (Nyquist plots). (c and d) Same as (a and b), respectively, 1 M $LiPF_6$ solutions.

of $ROCO_2Li$ or $ROCO_2M$ was formed for $LiNiO_2$ and $LiCoO_2$ aged at elevated temperatures in alkyl-based solutions [29]. This information is important for understanding the electrochemical results presented below.

Figs. 3 and 4 show cyclic voltammetry and EIS data (Nyquist plots) related to pristine and aged electrodes comprising $LiFePO_4$ synthesized by a sol–gel route, and measured/aged in $LiClO_4$ and $LiPF_6$ solutions at 30 and 60 °C (Figs. 3 and 4, respectively). It should be noted that this active mass demonstrated the highest stability (a very low iron dissolution, even in wet $LiPF_6$ solutions at 60 °C). The data presented in Fig. 3 related to 30 °C reflect a stable behavior upon storage in terms of both capacity and impedance. In general, capacities close to theoretical were obtained upon prolonged cycling or after weeks of aging, in both solutions. There is a question with respect to the use of impedance spectroscopy for insertion electrodes that undergo first-order phase transition during the course of their main redox activity, the latter being irreversible (as reflected by the hysteresis in the CV peaks of these electrodes, Fig. 3a and c). However, the high frequency response of impedance spectroscopy of these electrodes is always relevant. This part of the spectra reflects the fast processes: Li-ion migration through surface films, interfacial charge transfer, etc., which precede the much slower phase transition. As seen in all the EIS charts presented herein, the high frequency impedance of $LiFePO_4$ electrodes is lower as Li deintercalation proceeds (i.e., the highest for $LiFePO_4$ and the lowest for $FePO_4$). A clear feature of these electrodes is their higher impedance in $LiPF_6$ solutions, compared to that measured in $LiClO_4$ solutions. This result can be well explained by the formation of surface LiF (e.g., due to the reaction of $LiFePO_4$ with trace HF, which is always unavoidably present in $LiPF_6$ solutions [25]). LiF films are very resistive to Li-ion migration [29] and, thereby, their presence should increase the charge transfer resistance of Li insertion electrodes. This is in turn reflected by an increase in the high frequency semicircle in the Nyquist plots (Fig. 3b and d). The electrochemical behavior of these electrodes in wet $LiPF_6$ is similar to that in the dry solutions. However, their impedance in the wet solutions is at least twice as high. There is obviously a higher concentration of HF in the wet solutions, which will react quickly with $LiFePO_4$ to form resistive surface films comprising LiF.

Fig. 4 compares data from electrodes measured at 60 °C in $LiClO_4$ and wet $LiPF_6$ solutions (a, b and c, d respectively, as indicated). It is important to note that the electrochemical behavior of the sol–gel $LiFePO_4$ electrodes at 60 °C is similar to that measured at 30 °C. The full capacity can be obtained upon cycling, and the CVs reflect fast kinetics upon prolonged aging. As expected, the impedance of these electrodes is lower at 60 °C, as expected for activation-controlled, charge transfer behavior.

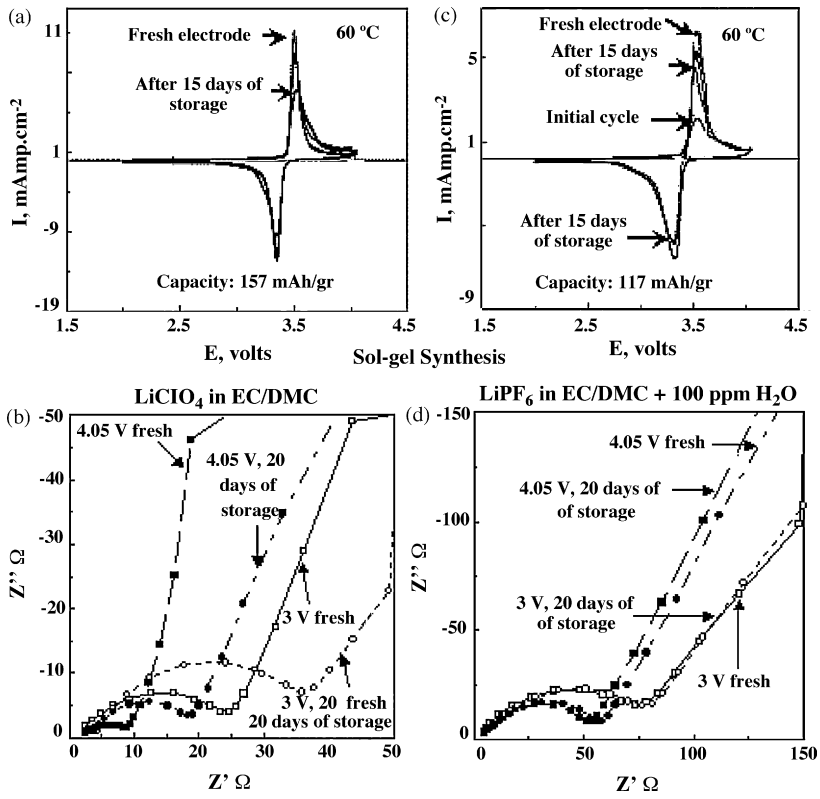

Fig. 4. Electrochemical data measured with electrodes comprising $LiFePO_4$ prepared by sol–gel synthesis, at 60 °C. (a) CVs of pristine and aged (15 days) electrodes in $LiClO_4$ solutions. Capacity and scan rate are indicated. (b) Impedance spectra (Nyquist plots) measured and 3 and 4.05 V (Li/Li^+) in $LiClO_4$ with pristine and aged (20 days) electrodes, as indicated. (c and d) Same as (a and b), respectively, 1 M $LiPF_6$ solutions containing 100 ppm H_2O.

The electrodes' impedance in $LiClO_4$ solutions increases during aging at 60 °C, which can be explained by the slow nucleophilic surface reactions between the negatively charged oxygen of the $LiFePO_4$ and EC molecules (which are highly electrophilic). As mentioned above, surface spectroscopic studies of $LiFePO_4$ electrodes showed evidence for the formation of surface species originating from reactions of the solvent molecules. The impedance of these electrodes in dry $LiPF_6$ solutions (not seen here) is twice as high as that in $LiClO_4$ solutions, while the impedance measured in wet $LiPF_6$ solutions at 60 °C may be five-fold higher than that measured in $LiClO_4$ solutions (see Fig. 4b and d), due to the formation of surface LiF in the $LiPF_6$ solutions, as explained above. However, the impedance of electrodes at 60 °C in the wet solutions is steady during storage. This results from the high reactivity of $LiFePO_4$ with solutions containing a relatively high concentration of HF at elevated temperatures, which leads to the quick formation of LiF films that then passivate the electrodes. Under such conditions, the electrodes' surface reaches a steady state during a short period of contact with the solution, and hence, further aging cannot lead to additional changes.

Figs. 5 and 6 relate to electrodes comprising $LiFePO_4$ prepared by solid-state synthesis, measured at 30 and 60 °C, respectively. Fig. 5 shows the impedance spectra of these electrodes measured in $LiPF_6$ and $LiClO_4$ solutions, as indicated. Upon aging at 30 °C in $LiPF_6$ solutions, the electrodes' impedance pronouncedly increases and is considerably higher that that measured in $LiClO_4$ solutions (see Fig. 5). The behavior of the electrodes comprising $LiFePO_4$ prepared by solid-state synthesis is quite different from the much more stable behavior of the electrodes made of $LiFePO_4$ synthesized by the sol–gel route. Fig. 6a and b presents data related to electrodes of

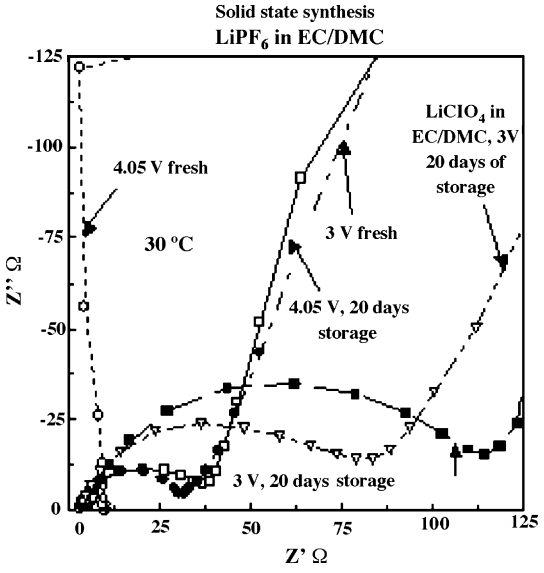

Fig. 5. Impedance spectra measured with pristine and aged (20 days) electrodes comprising LiFePO4 prepared by solid-state synthesis, at 30 °C in 1 M LiPF6 solutions, and at 3 and 4.05 V (Li/Li+), as indicated. A spectrum measured with a similar electrode at 3 V after 20 days of storage in LiClO4 solution (marked) is also presented for comparison.

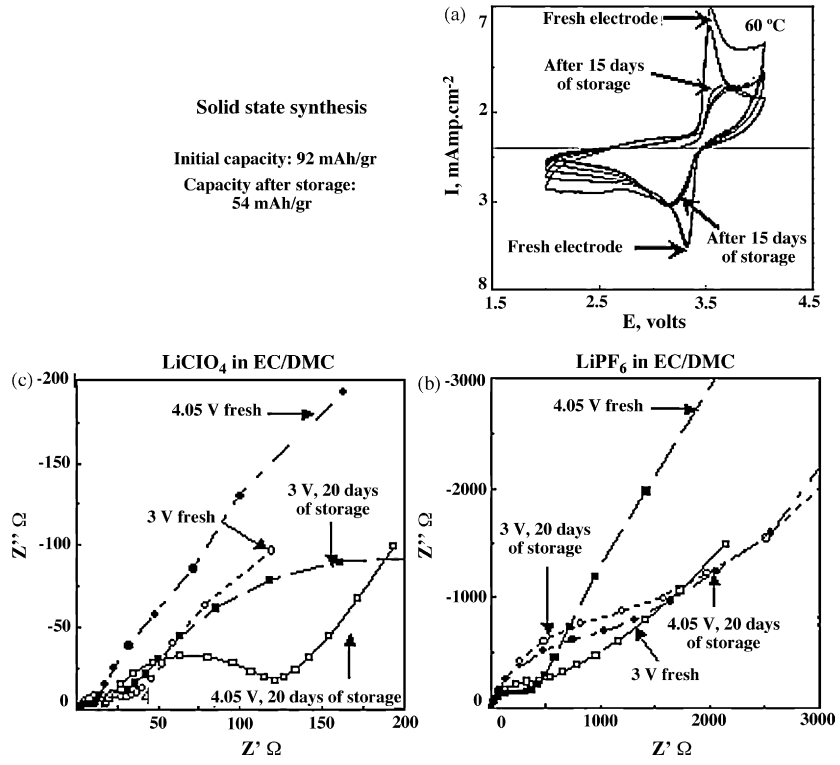

Fig. 6. Electrochemical data measured at 60 °C from electrodes comprising $LiFePO_4$ prepared by solid-state synthesis. (a) CVs of pristine and aged (15 days) electrodes in 1 M $LiClO_4$ solutions (capacity and scan rate are indicated). (b) Nyquist plots measured from pristine and aged (20 days) electrodes in 1 M $LiClO_4$ solutions at 3 and 4.05 V (Li/Li^+). (c) Same as (b), 1 M $LiPF_6$ solutions.

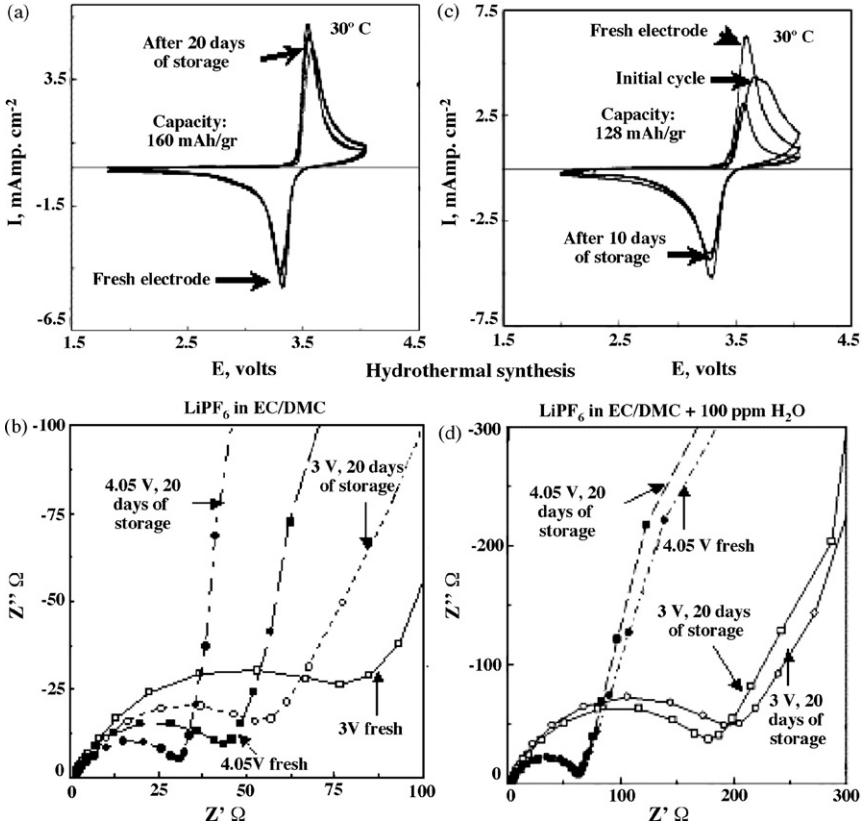

Fig. 7. Electrochemical data obtained at 30 °C with electrodes comprising $LiFePO_4$ prepared by hydrothermal synthesis. (a) CV of pristine and aged (20 days) electrodes measured in $LiPF_6$ solutions. Capacity and scan rate are indicated. (b) Nyquist plots measured in 1 M $LiPF_6$ at 3 and 4.05 V (Li/Li^+) with pristine and aged (20 days) electrodes, as indicated. (c and d) Same as (a and b), respectively, 1 M $LiPF_6$ solutions contaminated with 100 ppm of water.

solid-state synthesized $LiFePO_4$ measured at 60 °C in $LiPF_6$ solutions. There is a remarkable difference between the CV curves of this system, to those obtained with the same electrodes at 30 °C, or with electrodes comprising $LiFePO_4$ prepared by the sol–gel synthesis in all the solutions at both 30 and 60 °C.

The CVs presented in Fig. 6a have very broad peaks, which reflect sluggish kinetics. Upon aging, the CV peaks are even broader and reflect a lower capacity. The impedance spectra of this system (Fig. 6b) reflect very high surface impedance. The fact that the high frequency semicircles in the Nyquist plots thus obtained are incomplete, is a strong indication for the slow kinetics of these electrodes, due to impeded charge transfer. As seen in Fig. 6c, the impedance of these electrodes at 60 °C in $LiClO_4$ solutions, while increasing upon aging, is at least one order of magnitude lower than that measured in $LiPF_6$ solutions. The high frequency semicircles of the Nyquist plots all their regular, expected shapes (a closed loop).

Fig. 7 presents electrochemical data related to electrodes comprising $LiFePO_4$ prepared by hydrothermal synthesis measured in dry and wet $LiPF_6$ solutions at 30 °C. The capacity of these electrodes in dry $LiPF_6$ solutions is close to the theoretical one and does not fade upon aging. The impedance of these electrodes in dry $LiPF_6$ becomes lower upon aging and they show a much higher impedance in the wet solutions, which is only slightly affected by aging (see the explanation of the data presented in Fig. 4d). The capacity of these electrodes fades upon aging in the wet solutions (Fig. 7c).

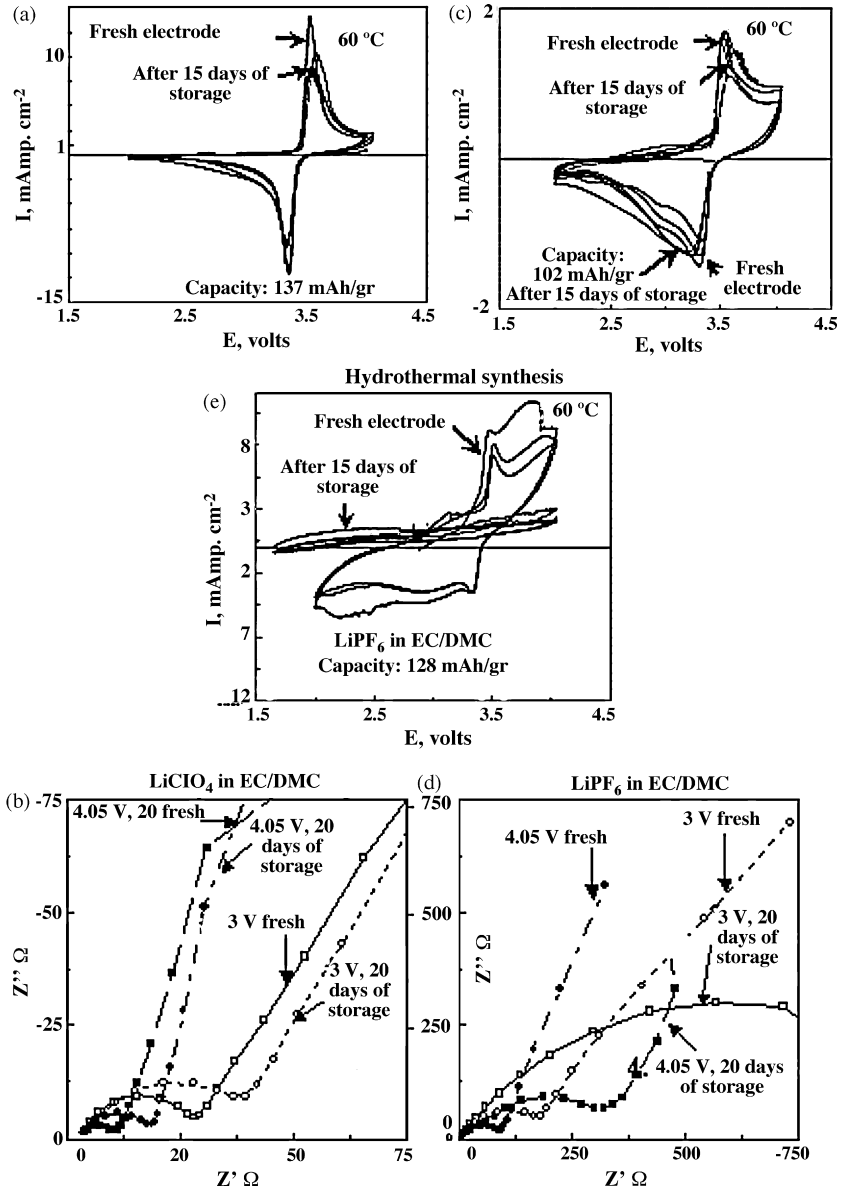

Fig. 8. Electrochemical data obtained at 60 °C with electrodes comprising $LiFePO_4$ prepared by hydrothermal synthesis. (a) CVs of pristine and aged (15 days) electrodes measured in 1 M $LiClO_4$ solutions. Capacity and scan rate are indicated. (b) Nyquist plots of pristine and aged (20 days) electrodes measured in 1 M $LiClO_4$ solutions at 3 and 4.05 V (Li/Li^+). (c and d) Same as (a and b), respectively, 1 M $LiPF_6$ solutions. (e) Same as (a and c), 1 M $LiPF_6$ solution containing 100 ppm of water.

Fig. 8 shows the electrochemical data related to these electrodes (hydrothermal synthesis) measured at 60 °C in $LiClO_4$ and in dry and wet $LiPF_6$ solutions, as indicated. These results reflect the pronounced effects of the solutions, as well as the significant difference between the behavior of these electrodes and that of the electrodes comprising $LiFePO_4$ prepared by sol–gel synthesis (compare Figs. 8 and 4). We attribute the broad CV peaks presented in this paper (e.g., Figs. 7 and 8) to surface phenomena which lead to development of high impedance and not to a possible existence of more then one extraction–insertion process (based on XRD measurements of aged materials). The behavior of these electrodes in $LiClO_4$ solutions at 60 °C can be considered as 'normal': sharp CV peaks that reflect initial capacity close to theoretical one and fast kinetics. Upon aging, some capacity fading may be observed. However, the basic electrochemical response of these electrodes remains steady (Fig. 8a). The impedance of these electrodes in the $LiClO_4$ solutions at 60 °C is, as expected, low, and increases slightly during storage (Fig. 8b). In contrast, their voltammetric behavior in dry $LiPF_6$ solutions reflects very sluggish kinetics, as demonstrated by the very broad peaks (Fig. 8c). The impedance of these electrodes is initially high (by one order of magnitude compared to that measured in $LiClO_4$ solutions), and remarkably increases upon storage (Fig. 8d). In the wet solutions, these electrodes show a very sluggish initial kinetics (very broad CV peaks), and completely lose their capacity on aging (Fig. 8e).

The results described above show the very strong influence of the synthetic mode of the olivine compounds on the stability and electrochemical behavior of their electrodes, especially at elevated temperatures. The difference in the electrochemical behavior of the electrodes in the various solutions correlates very well with the stability of these active materials in solutions upon storage, as reflected by iron dissolution. The material synthesized by the sol–gel reaction, that contains the highest fraction of iron phosphide on the surface shows the lowest rates of iron dissolution. This is true even in wet $LiPF_6$ solutions that can be considered as 'corrosive' for Li_xMO_y electrodes (M = transition metals such as Mn, Ni, Co). All the materials demonstrate stability in $LiClO_4$ electrolytes, even at elevated temperature (i.e., very low rates of iron dissolution). This correlates well with the fact that all three materials demonstrate normal electrochemical behavior and relatively low impedance in $LiClO_4$ solutions, even at 60 °C. The increase in the electrodes' impedance seen upon storage in $LiClO_4$ solutions at 60 °C is inevitable, and relates to possible reactions between the $LiFePO_4$ and the alkyl carbonate solvents. Hence, the stability of $LiFePO_4$ electrodes and their electrochemical performance depends strongly on the possible presence of acidic species in the solutions, which is unavoidable when the salt is $LiPF_6$, especially, when the solutions are contaminated by trace water.

4. Conclusion

$LiFePO_4$ electrodes demonstrate high stability at elevated temperatures, in solutions that contain no acidic or protic contaminants. In $LiPF_6$ solutions, which unavoidably contain trace HF, $LiFePO_4$ electrodes are stable at 30 °C, but can also be unstable at elevated temperatures, especially if the solutions are H_2O contaminated. The stability of $LiFePO_4$ electrodes in the 'corrosive' solutions, e.g., wet $LiPF_6$ solutions, definitely depends upon the synthetic route, and conditions used for processing. In this study, we found $LiFePO_4$ synthesized by a sol–gel method to be very stable in $LiPF_6$ solutions at elevated temperatures, possibly due to higher iron phosphide content on the surface. There is a very strong correlation between stability measured by the rates of iron dissolution upon storage and the electrochemical performance of $LiFePO_4$ electrodes. In systems (electrodes/solutions/temperatures) in which iron dissolution is significant, the electrodes' impedance is high and increases upon aging. The kinetics are sluggish and the capacity fades. The electrode's impedance is the highest in wet $LiPF_6$ solutions, and much higher in $LiPF_6$ solutions than in $LiClO_4$ solutions. This can be explained by the formation of highly resistive LiF surface films, due to reactions between $LiFePO_4$ and HF traces, which are present in $LiPF_6$ solutions. Since capacity fading upon aging at 60 °C was also found for electrodes and solutions that showed very low iron dissolution rates (e.g., $LiFePO_4$ synthesized by a hydrothermal route at $LiClO_4$ solutions), we suggest that capacity losses of Li_xFePO_4 electrodes do not necessarily result from bulk changes in the active mass, but rather from surface phenomena. For instance, surface film formation, when is intensive, can lead to the electrical isolation of particles, thus excluding them from the electrode's electrochemical activity. These studies show that the stability and very high performance of $LiFePO_4$ electrodes can be achieved by the appropriate choice of synthetic mode, processing conditions, and uncontaminated solutions.

Acknowledgments

A partial support for this work was obtained by the Israel Science Foundation (ISF).

References

[1] A.R. Armstrong, P.G. Bruce, Nature 381 (1996) 499.
[2] Y. Takeda, K. Nakahara, M. Nishijima, N. Imanashi, O. Yamamoto, M. Takano, Mater. Res. Bull. 29 (1994) 659.
[3] A.K. Pahdi, K.S. Nanjundaswamy, C. Masquelier, S. Okada, J.B. Goodenough, J. Electrochem. Soc. 144 (1997) 1609.
[4] A.K. Padhi, K.S. Nanjundaswamy, J.B. Goodenough, J. Electrochem. Soc. 144 (1997) 1188–1194;
J.B. Goodenough, A.K. Padhi, C. Masquelier, K.S. Nanjundaswamy, U.S. Patent 08/840,523 (1997).
[5] G. Li, H. Azuma, M. Tohda, Electrochem. Solid-State Lett. 5 (2002) A135.
[6] H. Huang, S.-C. Yin, T. Kerr, L.F. Nazar, Adv. Mater. 14 (2002) 1525;
J. Barker, M.Y. Saidi, U.S. Patent 5,871,866 (1999);
M.Y. Saïdi, J. Barker, H. Huang, G. Adamson, Electrochem. Solid-State Lett. 5 (2002) A149;
S.C. Yin, P. Strobel, M. Anne, L.F. Nazar, J. Am. Chem. Soc. 125 (2003) 10402.
[7] J. Barker, M.Y. Saidi, J.L. Swoyer, J. Electrochem. Soc. 150 (2003) A1394;
J. Barker, M.Y. Saidi, J. Swoyer, U.S. Patent 6,387,568 (2002);
J. Barker, M.Y. Saidi, J.L. Swoyer, Electrochem. Solid-State Lett. 6 (2003) A1.
[8] A. Alberti, G. Vezzalini, Zeit. Fur Kristallographie. 147 (1978) 167–175.

[9] M.S. Whittingham, Y. Song, S. Lutta, P.Y. Zavalij, N.A. Chernova, J. Mater. Chem. 15 (2005) 3362.
[10] F. Zhou, K. Kang, T. Maxisch, G. Ceder, D. Morgan, Solid State Commun. 132 (2004) 181.
[11] T. Maxisch, F. Zhou, G.G. Ceder, Phys. Rev. B 73 (2006) 104301.
[12] N. Ravet, Y. Chouinard, J.F. Magnan, S. Besner, M. Gauthier, M. Armand, J. Power Sources 97 (2001) 503;
N. Ravet, M. Armand, U.S. Patent Application 0195591A1 (2002).
[13] H. Huang, S.C. Yin, L.F. Nazar, Electrochem. Solid-State Lett. 4 (2001) A170.
[14] F. Croce, A. D'Epifanio, J. Hassoun, A. Deptula, T. Olczac, B. Scrosati, Electrochem. Solid-State Lett. 5 (2002) A47.
[15] D. Morgan, A. Van der Ven, G. Ceder, Electrochem. Solid-State Lett. 7 (2004) A30.
[16] Y.-I. Jang, B.J. Neudecker, N.J. Dudney, Electrochem. Solid-State Lett. 4 (2001) A74.
[17] A. Yamada, Y. Kudo, K.-Y. Liu, J. Electrochem. Soc. 148 (2001) A1153.
[18] V. Srinivasan, J. Newman, J. Electrochem. Soc. 151 (2004) A1517.
[19] A. Yamada, H. Koizumi, N. Sonoyama, R. Kanno, Electrochem. Solid-State Lett. 8 (2005) A409.
[20] A. Yamada, H. Koizumi, S.-I. Nishimura, N. Sonoyama, R. Kanno, M. Yonemura, T. Nakamura, Y. Kobayashi, Nat. Mater. 5 (2006) 357.
[21] C. Delacourt, P. Poizot, J.-M. Tarascon, C. Masquelier, Nat. Mater. 4 (2005) 254.
[22] B. Ellis, L. Perry, D. Ryan, L.F. Nazar, J. Am. Chem. Soc. 128 (2006) 11416.
[23] Y.-H. Rho, L. Perry, D. Ryan, L.F. Nazar, J. Electrochem. Soc. 154 (2007) A283.
[24] D. Aurbach, B. Markovsky, A. Rodkin, E. Levi, Y.S. Cohen, H.-J. Kim, M. Shmidt, Electrochim. Acta 47 (2002) 4291.
[25] R. Oesten, U. Heider, M. Schmidt, Solid State Ionics 148 (2002) 391.
[26] E. Zinigrad, L. Larush-Asraf, J.S. Gnanaraj, M. Sprecher, D. Aurbach, Thermochim. Acta 438 (2005) 184.27.
[27] E. Markevich, G. Salitra, D. Aurbach, Electrochem. Commun. 7 (2005) 1298.
[28] M. Koltypin, B. Ellis, L. Nazar, D. Aurbach, Electrochem. Solid State Lett. 10 (2007) A40.
[29] D. Aurbach, K. Gamolsky, B. Markovsky, G. Salitra, Y. Gofer, J. Electrochem. Soc. 147 (2000) 1322.